OPTIMIZATION OF PEDOT: PSS THIN FILM FOR ORGANIC SOLAR CELL APPLICATION

YURAIMY YAKIMIN BIN ABDUL TALIB

A project report submitted in partial
fulfillment of the requirement for the award of the
Degree of Master of Electrical Engineering

Faculty of Electrical and Electronic Engineering
UniversitiTun Hussein Onn Malaysia

JANUARY 2014

ABSTRACT

As a clean and renewable energy source, the development of the organics solar cells is very promising due to the inorganic solar cell inconvenient production process and material shortness. In this work, P3HT: PCBM bulk-heterojunction devices were produced by spin coating organic layers onto ITO coated glass in air, and deposited it with an Au layer as top metal electrode. Inverted devices were fabricated with and without PEDOT:PSS. Then, several attempts have been conducted to improve power conversion efficiency by optimizing different thicknesses of the interlayer between active layer and metal. Power conversion efficiency, short circuit current, open circuit voltage and fill factor were measured on all produced devices. In contrast, the devices with 50 nm thickness of PEDOT: PSS layer showed as better solar cell with 0.0394% efficiency compared to the devices without PEDOT:PSS. As a result, introduction of PEDOT:PSS layer on active layer improves hole collection at the metal / active layer interface.

ABSTRAK

Sebagaisumbertenaga yang bersihdanbolehdiperbaharui, pembangunanorganiksel solar berasaskan material organic adalahsangatcerahberbandingsel solar berasaskan material tidak organic seperti Silicon yang perlumengharungi prosespengeluaran yang menelankos yang tinggi. Dalamlaporanprojekini, sel yang berasaskan material organic P3HT: PCBM dihasilkandenganmenitiskanbahantersebutkekaca ITO bersalutmelalui proses putaranberhalajatinggi, danseterusnyadidepositkandenganlapisanemassebagaielektrodlogamatas.Selberstrukturbaru di hasilkansamadadenganlapisan PEDOT:PSSataupunsebaliknya. Kemudian, beberapapercubaantelahdijalankanuntukmeningkatkankecekapanpenukarankuasacahayakepadakuasaelektrikdenganmengoptimumkanketebalan yang berbezaantaralapisanaktifdanlogam.Untuktujuanitu, beberapa parameter pentingberkaitankecekapansel solar tersebuttelahdikajidandiukur.Perantidenganketebalan 50nm lapisan PEDOT: PSS merupakansel solar yang lebihbaikdengankecekapan 0.0394% berbandingdenganperantitanpalapisan PEDOT: PSS. Hasilnya, pengenalanlapisan PEDOT: PSS padalapisanaktifmemperbaikipenghasilancasantaralapisanaktifdanlogam.

CONTENTS

TITLE		**i**
DECLARATION		**ii**
DEDICATION		**iii**
ACKNOWLEDGEMENT		**iv**
ABSTRACT		**v**
CONTENTS		**vii**
LIST OF TABLES		**x**
LIST OF FIGURES		**xi**
LIST OF SYMBOLS AND ABBREVIATIONS		**xii**
LIST OF APPENDIX		**xiii**
CHAPTER 1 INTRODUCTION		**1**
1.1	Background	2
1.2	Problem statement	4
1.3	Objective	4
1.4	Scope of the project	4
1.5	Report project outline	5

CHAPTER 2 FUNDAMENTAL OF ORGANIC SOLAR CELL 6

2.1 Charge generation of organic solar cell 6
2.2 Characterization of organic solar cell 9
2.3 EquivalentCircuit Diagram 9
2.3.1 Open circuit voltage (V_{OC}) 11
2.3.2 Short circuit density, current (J_{SC}, I_{SC}) 11
2.3.3 Fill factor FF 11
2.3.4 Power conversion efficiency PCE (η) 12

CHAPTER 3 CELL FABRICATION & TESTING 13

3.1 Energy level of device fabrication 14
3.2 Material 15
3.2.1 ITO 15
3.2.2 P3HT:PCBM 16
3.2.3 PEDOT:PSS 17
3.3 Substrate and material preparation 18
3.3.1 ITO etching and cleaning 18
3.3.2 P3HT:PCBM solvent preparation 19
3.3.3 PEDOT:PSS preparation 20
3.4 Fabrication of reference cell 22
3.5 Fabrication of cell with PEDOT:PSS 25
3.6 Fabrication tool 26
3.7 Device characterization 30

CHAPTER 4 RESULT AND DISCUSSION 34

4.1 PEDOT:PSS filtration effect 34
4.2 Surface topography of PEDOT:PSS 35
4.3 Thickness profile of PEDOT:PSS 36
4.3.1 Spin speed dependence thickness profile 36
4.3.2 Drop volume dependence thickness profile 37
4.4 I-V measurement result 39
4.4.1 Reference device 39

4.4.2 Devices with PEDOT:PSS 41

CHAPTER 5 CONCLUSION AND FUTURE WORK 45

REFERENCES 47

LIST OF TABLES

4.1	Spin-drop and drop-spin comparison	37
5.2	Device performance under 1.5AM	44

LIST OF FIGURES

1.1	Basic principle of organic solar cell	1
2.1	Fundamental mechanism of charge generation	6
2.2	Ideal structure of bulk heterojunction solar cell	7
2.3	Energy level of molecular	8
2.4	Simplified example of LUMO-HOMO charge generation	8
2.5	The equivalent circuit diagram of solar cell	9
2.6	Typical I-V characteristic of OSC under dark and illumination condition	10
3.1	The schematic of inverted organic solar cell	13
3.2	Ideal energy level diagram for OSC	14
3.3	Schematic illustration of conventional and inverted device structure	15
3.4	Molecular structure of P3HT PCBM	16
3.5	Molecular structure of PEDOT doped with PSS	17
3.6	Graphical image of etched substrate	18
3.13	Cross section of reference cell	22
3.17	Cross section of device with PEDOT:PSS	25
4.1	AFM captured imaged of PEDOT:PSS	34
4.2	AFM topography of PEDOT:PSS	35
4.3	Spin speed dependence PEDOT:PSS	36
4.6	I-V Characteristic of reference cell	39
4.7	Power curve of reference cell	40
4.8	I-V Characteristic of device with PEDOT:PSS	41
4.9	Power curve of cells	44

LIST OF SYMBOLS AND ABBREVIATIONS

OSC	-	Organic solar cell
P3HT	-	Poly (3-hexylthiophene)
PCBM	-	[6, 6]-phenyl C_{61} -butyric acid methyl ester
PEDOT	-	poly (3, 4-ethylenedioxythiophene)
PSS	-	poly (styrenesulfonate acid)
ITO	-	Indium tin oxide
HOMO	-	highest occupied molecular orbital
LUMO	-	lowestunoccupied molecular orbital
AM	-	Air mass
Au	-	Gold
Al	-	Aluminium
V_{OC}	-	Open circuit voltage
I_{SC}	-	Short circuit current
FF	-	Fill factor
PCE (η)	-	Power conversion efficiency
I_L	-	Current source
R_{SH}	-	Shunt resistor
R_S	-	Series resistor
I_0	-	Dark saturation current
n	-	Diode ideality factor
I_L	-	Light generated current
V_{max}	-	Maximum voltage
I_{max}	-	Maximum current
P_{IN}	-	Input power

CHAPTER 1

INTRODUCTION

Organic solar cells (OSC) represent a promising technology with tremendous potential for renewable energy at very low cost and abundant materials. OSC cells also play a significant role as a zero-emission source of energy during the power generation process.

The photovoltaic definition of OSC can be described as a process of converting solar light (photon) to electricity (voltage). In OSC cells, the structure of the cell can be categorized into two: (i) the conjugated polymers and (ii) the small organic molecules. The conjugated polymers also are known as bulk-heterojunction solar cells, where the mechanism of the electricity generation is dependent on the electron donor and acceptor inside the polymers. OSC cells are distinguished from the inorganic photovoltaic cells such as silicon-based by its major materials and electrical operation. The efficiency of inorganic solar cells can reach 20% while the best OSC based on bulk-heterojunction structure operate at 3-5% efficiency.

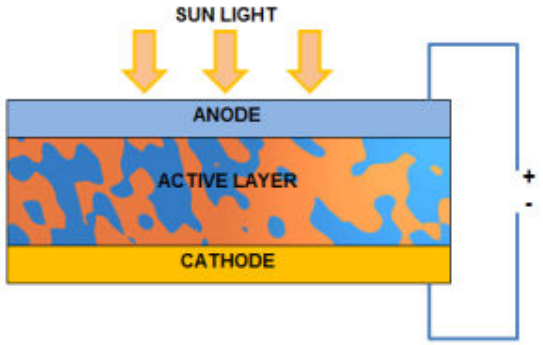

Figure 1.1: Basic principle of organic solar cell

1.1 Background to the study

In 1839, Alexander-Edmund Becquerel discovered the photovoltaic effect while studying the effect of light on electrolytic cells [1]. He found that electricity can be generated by illuminating an electrode with different types of lights. He also found a use for the photovoltaic effect by developing an "actinograph" which was used to record the temperature of heated bodies by measuring the emitted light intensity.

Further in 1876, the first demonstration of the photovoltaic effect in an all solid state system was reported by Adam and Day [2]. The report concluded that by inducing light to the selenium bar, crystallization of the outer layer of the bar produce an electric current. However, it was found that the electric current produced through the bar was weak.

In 1941, inorganic photovoltaic device based on junction separation were described [3]. Light exposed to the silicon junction stimulated electrons to flow from the n-side and p-side, resulting in an electric current. Meanwhile, development of inorganic photovoltaic using several techniques to form junction resulted in the announcement of the first modern solar cells in 1954 by Chapin, Fuller and Pearson [4]. It was silicon based with an efficiency of 6%. Over 50 years, silicon based solar cells has reached an efficiency of over 25%, with various configuration and material structure has been carried out [5]. However, efforts and approaches to reduce the cost of the high efficiency of inorganic solar such as Si has becoming very difficult and complicated due to the limitation of the technology itself. Due to this, recent researches are driven to explore the chemical flexibility for modifications in organic semiconductors.

Organic semiconductors are less expensive alternative than inorganic semiconductors. Organic molecules can be processed by large number of cheap processing techniques as the organic materials are available in our modern society. In 1983, the first generation of the organic photovoltaic was based on single organic layer sandwiched between two metal electrodes of different work functions. G.A Chamberlain has reported the conversion efficiencies in sunlight were generally poor (in the range of 10^{-3}% to 10^{-2}%) [6].

The next breakthrough was in 1986 when Tang reported about 1% efficiency for two organic materials. He introduced the p-n heterojunction concept, in which

two organic layers with hole and electron conducting properties were sandwiched between electrodes [7]. However, he suggested that the interface between organic/electrode is crucial in determining the solar cells properties. To overcome this problem, Saricifici in 1992 had prepared the active layer of conjugated polymer/fullerene composite with p-conjugated polymer as donor and fullerene as acceptor [8]. In 1995, an improved configuration known as bulk-heterojunction was introduced by Yu and Heeger. They observed that photoconductivity in the conjugated polymers was highly increased [9].

Despite their low efficiency, the Poly (3-hexylthiophene) (P3HT) and [6, 6]-phenyl C_{61} -butyric acid methyl ester (PCBM) bulk-heterojunction blends is one of the promising organic solar cells materials [10]. Today, it has been considered as the most efficient fullerene based donor-acceptor so far, yielding above 3.5% efficiency [11]. Several improvement of efficiency of organic solar cells has been made, and the achieved efficiency has evolved from less than 1% to 6%, as reported recently [12].

The race to improve the organic solar cells is however, inherited a major drawback of the organic material origin. They easily degrade under environmental conditions due to humidity, oxygen and light [13]. An additional layer between electrode and active layer has been introduced by using poly (3, 4-ethylenedioxythiophene): poly (styrenesulfonate acid) (PEDOT: PSS) to enhance stability while improving selectivity of the anode, facilitated hole transportation and to limit the recombination, hence increasing the cell efficiency [14][15][16].

However, the optimization of the thickness of the hole transport layer of PEDOT: PSS on active layer of P3HT: PCBM is still not clear, partly understood and subject of further study.

1.2 Problems Statement

It's been reported that the electron-hole transport efficiency is crucial to the OSC's overall performance, while the introduction of uniform interfacial contact can reduce the leakage current.

Current studies also suggested that buffer layers are needed as transportation method in order to reduce the potential contact between P3HT: PCBM (active layer) and Indium Tin Oxide (ITO), as well as the prominent contact layer of metal. Due to the large band gap between the work function of ITO and the highest occupied molecular orbital (HOMO) of the active layer, recombination can occur at the interface, causing the photoconductivity of the device to decrease [17].

The thickness of the PEDOT: PSS as HTL remain as a questionable topic whether the diffusion of exciton of the light photon could travel along; improve the charge extraction, associate with the device efficiency.

1.3 Objective

The aim of this project is to optimize, characterize and test the PEDOT: PSS as the hole transport layer by using sol-gel method to improve organic solar cells efficiency. This aim is based with following objectives:

(i) To study the effect of different thickness of PEDOT:PSS layer on OSC efficiency

(ii) To compare the electrical performance between different thicknesses

1.4 Scope of the project

This particular project focuses on the fabrication and characterization of bulk-heterojunction solar cell, incorporate with optimization the thickness of PEDOT:PSS as hole transport layer between active layer and metal electrode. Key factors as following scopes will be discussed.

(i) To explore and understand thoroughly the principle of basic OSC device structure and the role of PEDOT:PSS through literature review and background study

(ii) To identify the type of filtration needed for aqueous PEDOT: PSS.

(iii) To fabricate and characterize basic OSC device without PEDOT: PSS of ITO/P3HT: PCBM/AU structure.

(iv) To characterize and optimize OSC device of ITO/ /P3HT:PCBM/PEDOT: PSS AU structure with different thicknesses of PEDOT: PSS.

(v) To test the OSC device electrically under 1.5AM illumination using solar simulator system.

1.5 **Project report outline**

This project report consists of 5 main chapters, and organized as follows: Chapter 2 brief overview of organic solar cell and explanation on mathematical theory of solar cell. Electrical characterization for standard OSC devices will be also included in this chapter. Chapter 3 describes material and experimental methods involved in this project. Chapter 4 describes process optimization result and electrical characterization of OSC for introducing PEDOT:PSS as hole transport buffer layer. Chapter 5 provides a conclusion and future work as well as recommendation.

CHAPTER 2

FUNDAMENTAL OF BULK HETEROJUNCTION OSC

2.1 Charge generation of organic solar cell

As described briefly in previous introduction in Chapter 1, bulk heterojunction solar cell is a polymer blend, normally produced by mixing electron donor and electron acceptor material. The mechanism of charge generation in polymer active layer is shown in Figure 2.1[18].

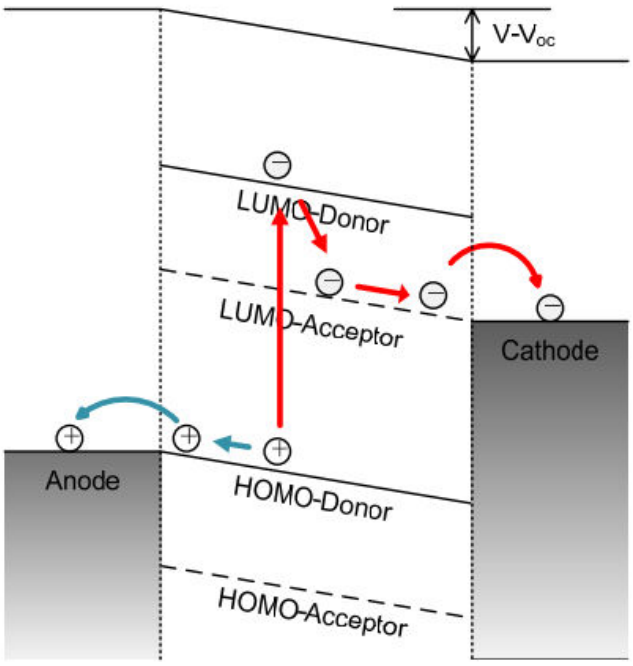

Figure 2.1: Fundamental mechanism of charge generation.

First, the oscillating electric field of light incident photon travel along to its wavelength. A conjugated polymer absorbs those photons to generate an electron-hole pair, also known as exciton. In bulk heterojunction active layer, most of the generated exciton blends in the donor polymer. Excitons diffuse to the interface of the donor and acceptor, where electrons travel from the LUMO level of the donor to the LUMO level of the acceptor. HOMO and LUMO are analogous to the valence and conduction bands of inorganic semiconductors. The energy difference between theHOMO and LUMO level is regarded as the band gap energy corresponding to the minimum photon energy photon in the light absorption.

This electrons transfer process also known as dissociation of exciton with generation of charge. Subsequent to charge separation, free holes and electrons migrate away from the donor acceptor interface and exit through the anode and cathode contacts [18].

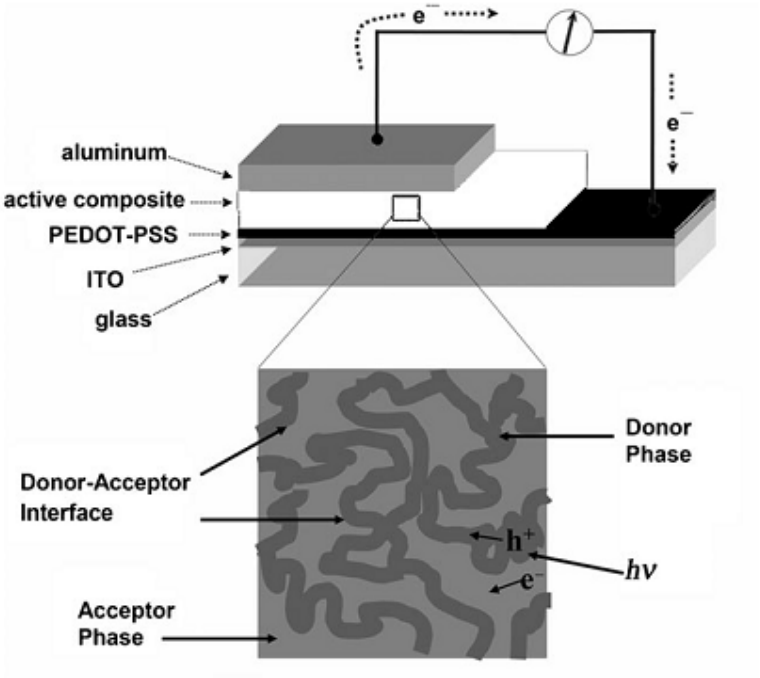

Figure 2.2: Ideal structure of bulk heterojunction solar cell, with a magnified area showing morphology of conjugated donor-acceptor polymer blend.

Further explanation on excitons molecular orbital is described as Figure 2.3. In ground state, the lowest energy is required to excite an electron in the HOMO to the lowest LUMO [19]. In OSC, the energy offset between LUMO of donor and acceptor more than 0.3 eV is required to provide sufficient electric field to assist in exciton dissociation.

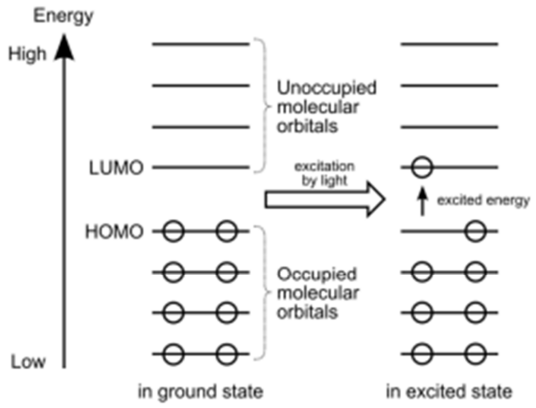

Figure 2.3: Energy level of molecular

The conversion of electrical energy from light energy in OSC as mentioned above can be summarized as Figure 2.4.

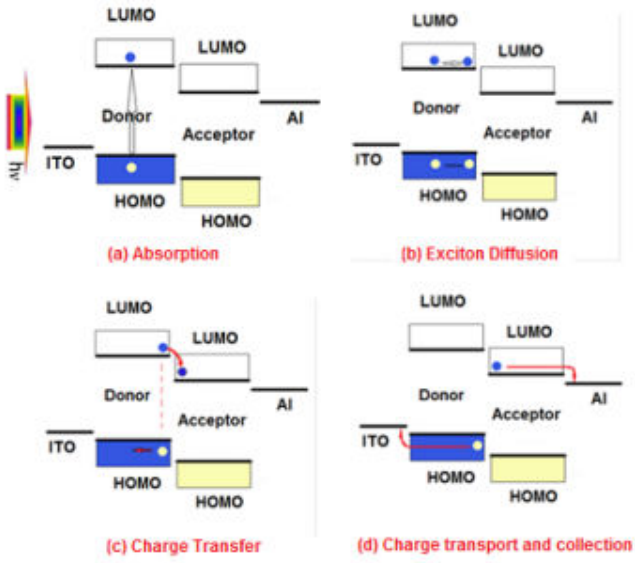

Figure 2.4: Simplified example of LUMO-HOMO charge generation in heterojunction structure [18].

2.2 Characterization of organic solar cell

I-V measurement is the most popular method for solar cell characterization. Important information about the solar cell performance can be determined through this method. By understanding the root of the method may lead to further optimization of the parameter involved.

I-V characteristic of the OSC is largely dependent to the material and interface's conductivity, exciton recombination, exciton diffusion length, electron-hole collection at electrode as well as light absorption. Those elements may affect the open circuit voltage V_{OC} and short circuit current I_{SC} while poor charge collection decreases the fill factor FF [20]. From all given parameters, the device capability to convert the incident light into electrical power can be determined as power conversion efficiency (η).

2.3 Equivalent Circuit Diagram

The equivalent circuit of a solar cell consists of current source (I_L), ideal diode and two parasitic resistors; shunt resistor (R_{SH}) and series resistor (R_S) respectively, as shown in Figure 2.5.

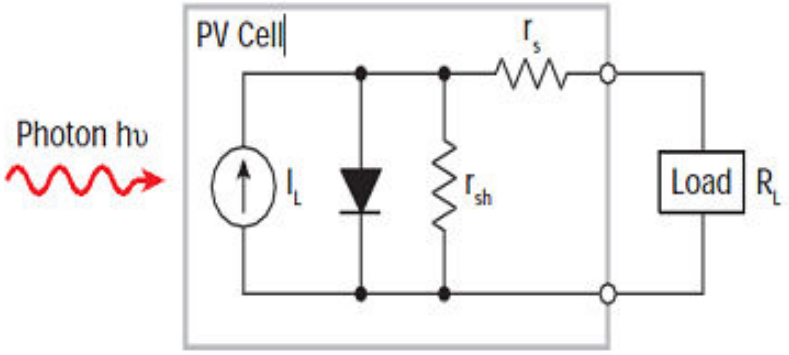

Figure 2.5: The equivalent circuit diagram of solar cell

The current source (I_L) represents the generated current energy from light photon (hv). The circuit's I-V characteristic equal to ideal diode only when series resistor R_S vanishes and the shunt resistor R_{SH} becomes infinity. Practically, the

$R_S$value is not zero due to the resistance of the organic material, the interlayer contact resistance and the metal electrode resistance whiles the R_S value depends to the charge carrier recombination at the surface of the donor-acceptor junction.

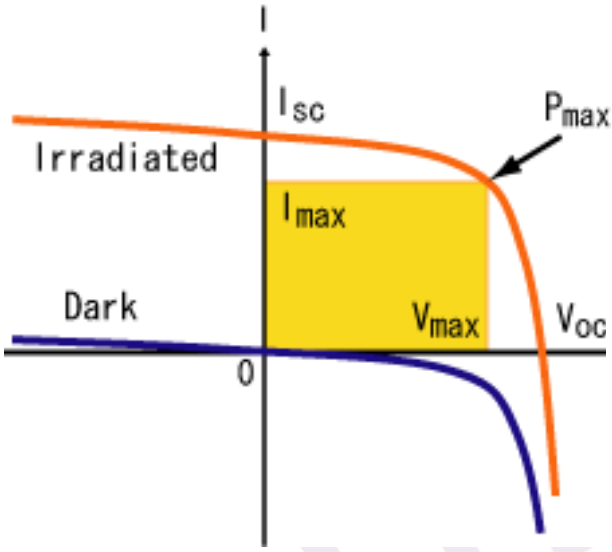

Figure 2.6: Typical I-V characteristic of OSC under dark and illumination condition.

The common parameters of an OSC can be derived from J-V characteristic, such as V_{OC}, I_{SC}, FF and PCE as shown in Figure 2.6. During dark condition (blue line), the I-V curve is an ideal characteristic of a diode, there will be zero power generated, which is determined as a maximum square form in the I-V curve (yellow area). In contrarily, during illumination, the light has the effect of shifting the I-V curve as the cell begins to generate power. The equation for the I-V curve is defined so that

$$I = I_L - I_0\left[\exp\left(\frac{qV}{nkT}\right)\right]$$

whereI_0 is the dark saturation current, *n* is the diode ideality factor and $I_L$is the light generated current It is clear that the greater the light intensity, the greater the amount of shift [21].

2.3.1 **Open circuit voltage (V_{OC})**

V_{OC} is the voltage under open circuit conditions. If the contacts between the organic and both electrodes are Ohmic, it will influence the V_{OC} since V_{OC} is determined by the energy difference between HOMO level of donor and the LUMO level of acceptor [22]

$$V_{OC} = \frac{1}{e}\left(E_{HOMO-donor} - E_{LUMO-acceptor}\right) + C$$

where C is an empirical constant that concerned to the dark I-V curve of diode.

2.3.2 **Short circuit current density, current (J_{SC}, I_{SC})**

I_{SC} is the current through the solar cell when there is no applied bias to the cell. $I_{SC}$is highly related to the charge generation, collection and transportation to both electrodes as mentioned above in sub chapter 2.2. When comparing solar cells with difference area of cell, it is beneficial to convert current I_{SC} to current density J_{SC}.

2.3.3 **Fill factor FF**

The next derivative parameter is fill factor FF that represents the ratio of maximum square area power to the product of V_{OC} and I_{SC}. Graphically, the FF is a measure of how "square" the solar cell fit to the I-V curve as shown in above figure 2.6. The FF is commonly determined from the measurement of the I-V curve and is defined as:

$$FF = \frac{P_{\max}}{V_{OC} I_{SC}} = \frac{V_{\max} I_{\max}}{V_{OC} I_{SC}}$$

whereV_{max} and I_{max} are the voltage and current at the actual maximum output power [23].

2.3.4 **Power conversion efficiencyPCE (η)**

The efficiency of a solar cell is determined as the fraction of light incident power which is converted to electricity. In other words, PCE is the ratio of the output power to the light power [24].

$$PCE\ \eta = \frac{P_{OUT}}{P_{IN}} = \frac{V_{OC} I_{SC} FF}{P_{IN}}$$

where P_{IN} is the input power under Standard Test Condition (100 W/cm^2, AM 1.5 (Air Mass) solar spectrums, temperature during measurements 25°C. In this project, the input power for an area of 0.16 cm^{2}cell was 0.016W.

CHAPTER 3

CELL FABRICATION & TESTING

The fabrication of each solar cell is accomplished by deposition of polymers and metal on ITO coated glasses. The each deposited layer range between 50 nm to 200 nm, making the devices vulnerable to being contaminated. Air and particle control were crucial during the fabrication process. The consequences of such contaminations were visible to the naked eye such as comet tail defect.

As for my work, the fabrication process was done under air controlled fume hood. The device structure of the solar cell is described in Figure 3.1. The scope of this design is limited to the inverted solar cell structure, where the ITO function as cathode, and the metal electrode as anode.

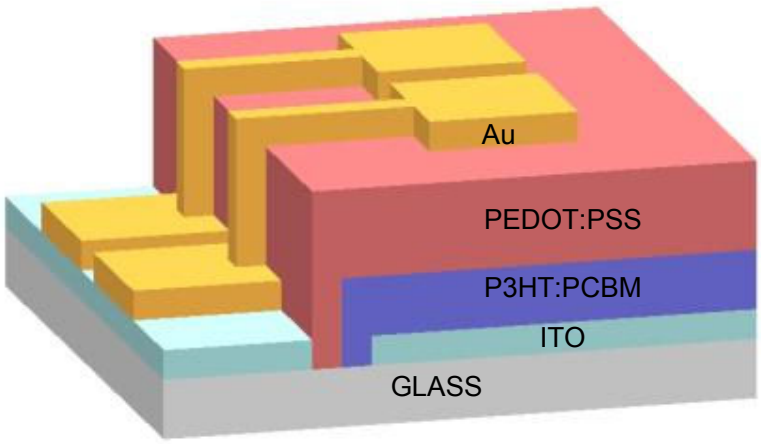

Figure 3.1: The schematic of inverted organic solar cell

3.1 **Energy level of device fabrication**

As mentioned earlier, this project will focus on inverted solar cell design structure. This design consists of a layer of active polymer layer thin film sandwiched between ITO and a metal electrode. The energy level diagrams of two designs in device fabrication are shown in Figure 3.2

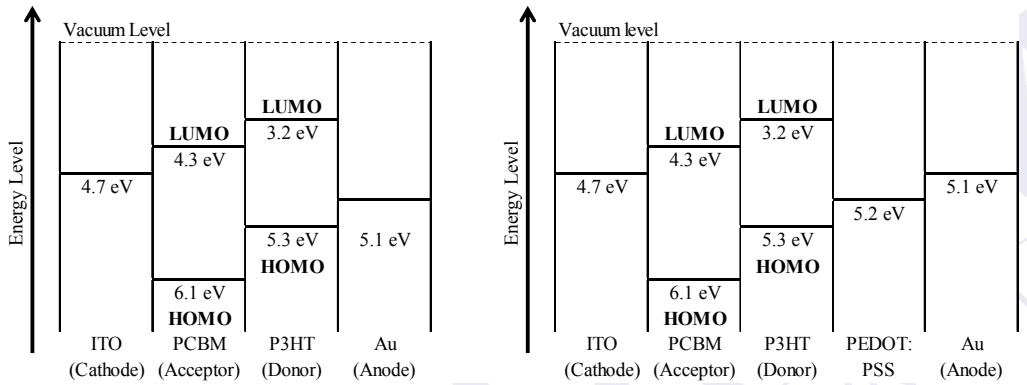

Figure 3.2: Ideal energy level diagram for OSC (a) reference device without PEDOT:PSS and (b) device with PEDOT:PSS layer. Note that the work function value is taken from literature [12][25].

The work function is the minimum energy needed to move an electron from the Fermi level to vacuum energy. The high value of work function of PEDOT:PSS is responsible in reducing the barrier height between metal electrode and active layer interface. Theoretically, the PEDOT:PSS layer is functioning as hole transport and electron block as well.

3.2 **Material**

Two types of OSC configuration were produced, one as a reference device without PEDOT:PSS and other devices with PEDOT:PSS layer thickness from 10 nm to 150 nm. Further, as for this project, an inverted structure of OSC was studied and fabricated. Comparison of both structures is shown as following Figure 3.3.

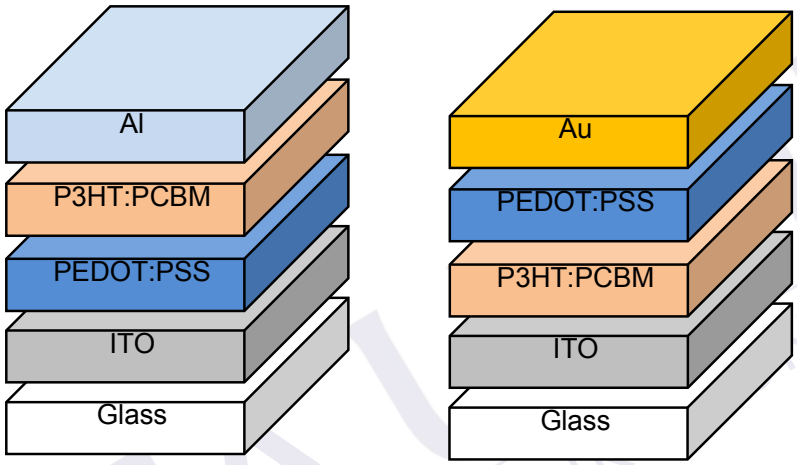

Figure 3.3: Schematic illustration of. (a) Conventional device structure and (b) Inverted device structue

3.2.1 **ITO**

Indium tin oxide (ITO) is colorless and transparent in thin layers, but it is yellowin bulk. Typically, ITO is grown on glass substrate. Because of its electrical conductive and opticaltransparent properties, it has become the most popular transparent conductive oxide. Again it can easily to be deposited which is another reason why it is used widely in thin film technology. ITO is a highly doped n -type semiconductor; its band gap is around 4eV [26].

3.2.2 **P3HT:PCBM**

The poly (3-hexylthiophene) (P3HT) and [6, 6]-phenyl C61-butyric acid methyl ester (PCBM) blend is the most efficient and well-studied material for OSC applications. It is the most efficient fullerene based derivate based donor-acceptor co polymer so far [11][27]

Their structures are as shown Figure 3.4. PCBM is a fullerene derivative. Because of high hole mobility, it plays the role of electron acceptor in many organic cells. P3HT is among thePolythiophene family,which is a conducting polymer. It is the excitation of the π-orbit electron in P3HT that gives the photovoltaic effect in the blend[28].

Both of the polymers were ordered from Sigma-Aldrich with 98% regioregularityof P3HT and 99% of PCBM in solid grade form.

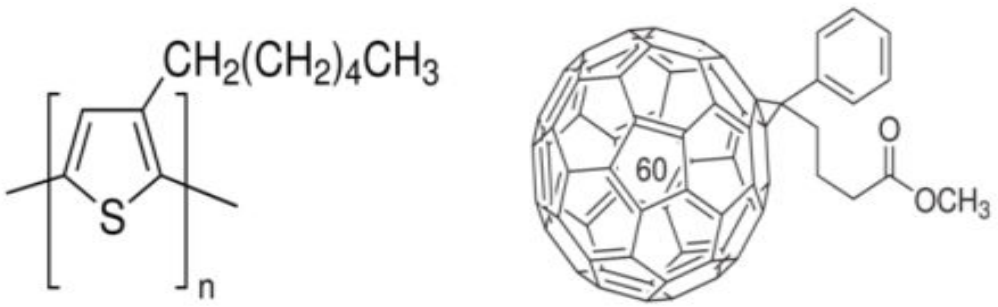

(a) (b)

Figure 3.4: Molecular structure of (a) P3HT (b) PCBM

3.2.3 **PEDOT:PSS**

PEDOT is the abbreviation of poly (3,4-ethylenedioxythiophene) and is one of many derivatives of the thiophenes. It is a conjugated polymer built from ethylenedioxythiophene (EDOT) monomers. PSS stands for poly (4-styrenesulfonate) and is also a polymer. PEDOT:PSS is the polymer mixture of both ionomers. It is conductive and water soluble. It can be cleaned by using organic solvent such as acetone and IPA. The chemical structure is shown in Figure 3.5.

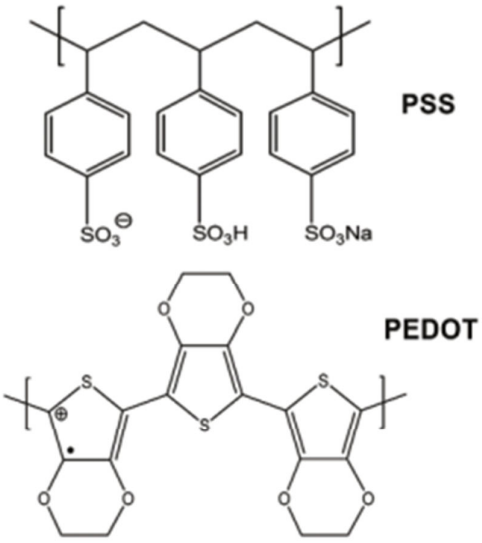

Figure 3.5: Molecular structure of PEDOT doped with PSS [29]

The PEDOT:PSS in this project is ordered from Sigma-Aldrich. It is conductive grade with PEDOT content of0.5 wt. %, PSScontent of 0.8 wt. %, concentration of 1.3 wt %, dispersion in water, band gap of 1.6 eV and conductivity of 1S/cm.

3.3 Substrate and material preparation

3.3.1 ITO etching and cleaning

The first step in the fabrication of each cell is preparing the as bought ITO coated glass substrate. The ITO coated glass with size of 2.5 cm x 2.5 cm and resistance of 15-25 ohm/sq was purchased from Sigma-Aldrich.

First the ITO side of the glass was covered with tape, while exposing small area on the other edges. The left side of Figure 3.6 shows the area where the ITO has been etched off. The substrate was placed in 40 % HF solution for approximately 60 sec. The conductivity of the etched and covered part of ITO was measured to ensure if the ITO had been completely etched. HCl and H2O mixed solution with the ratio of 1:5 also have been tested and capable to do the same etching process for approximately 15 minutes.

The patterned ITO was sonicated in acetone for 5 minutes and followed by thorough rinse with deionized water. Finally, a N2 dry gun purging completed the cleaning process. From this point forward, many precautions were taken to keep the substrates free from any dust or any other contaminant.

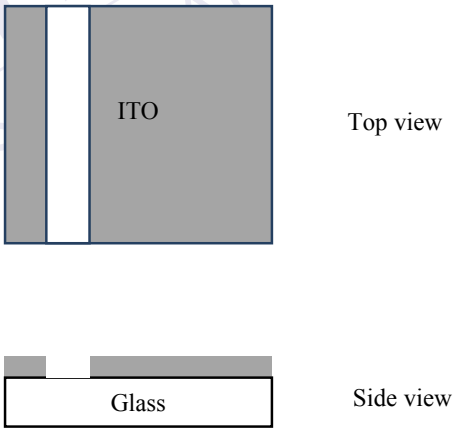

Figure 3.6: Graphical image of etched substrate, top and side view. Greyed area is the remaining ITO layer

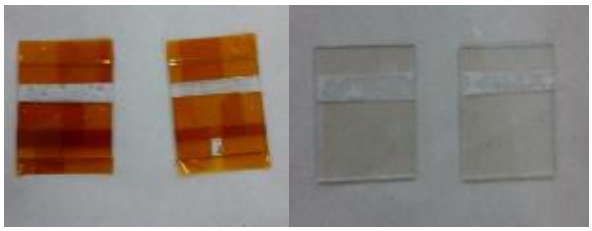

Figure 3.7: Actual images of etched ITO substrates. Left image showed that the patterning process was done using tape.

3.3.2 **P3HT:PCBM solvent preparation**

Firstly, solution was prepared by mixing15mg of poly (3-hexylthiopene)(P3HT)and 15mg of [6,6]- phenyl-C61 butyric acid methyl ester (PCBM) in a ratio of 1:1 in 1ml 1,2 Dichlorobenzene as a solvent.

Figure 3.8: 15mg poly (3-hexylthiopene) (P3HT)

Figure 3.9: 15mg [6, 6]- phenyl-C61 butyric acid methyl ester (PCBM)

Figure 3.10: 1ml 1, 2 Dichlorobenzene from Sigma-Aldrich

The mixture was then stirred together by using magnetic stirrer in a room temperature for 24 hours for ageing process before it can be used.

Figure 3.11: P3HT:PCBM Ageing process

3.3.3 **PEDOT: PSS preparation**

30 ml of PEDOT:PSS was taken out into a beaker by using plastic pipette from the bottle. Since the PEDOT:PSS was stored under cool condition around 2°C - 8°C, the aqueous solution of PEDOT:PSS was then stirred by using magnetic stirrer in a room condition. The stirring process was longed for 1 hour due to insoluble grains were observed during the experiment.

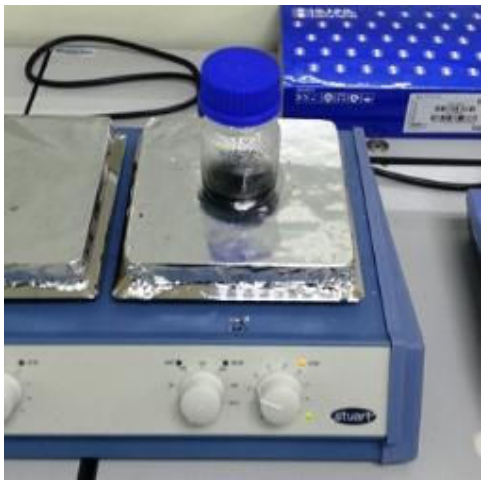

Figure 3.12: PEDOT:PSS stirred for 1 hour

3.4 Fabrication of reference cell

As mentioned earlier, a reference cell was produced with a basic structure of OSC, consisting of a sandwiched P3HT:PCBM active layer between ITO as a cathode and gold layer as an anode. See Figure 3.13.

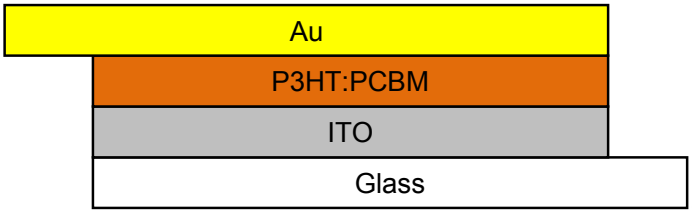

Figure 3.13: Cross section of a reference cell with PEDOT:PSS layer

First, the patterned ITO earlier was placed on the vacuum chuck of the spin coater. The mixture of the P3HT:PCBM solution was dropped onto the newly cleaned ITO substrate evenly, before spun with two steps spin speed. The first speed was set with lower speed of 500 rpm for 30 sec, continued with higher speed of 1000 rpm for 60 sec. The reason behind this was to keep the active layer spread evenly before dried up eventually. The desired range of thickness was 70 nm to 100nm layer.

After spin-coating, the edge of the P3HT:PCBM layer was wiped off to expose a small line of ITO anode by using a cotton bud was soaked with DI water. The cotton bud was dabbed on clean wiper first otherwise water can spread across the device and spoil the layer. The device was then immediately placed onto hot plate for 5 minutes at temperature 60°C to remove any water residue trapped within the blend as shown in Figure 3.14. Then, the device was placed onto cooling glass before placing the device in a sample holder with the lid closed to avoid any dust.

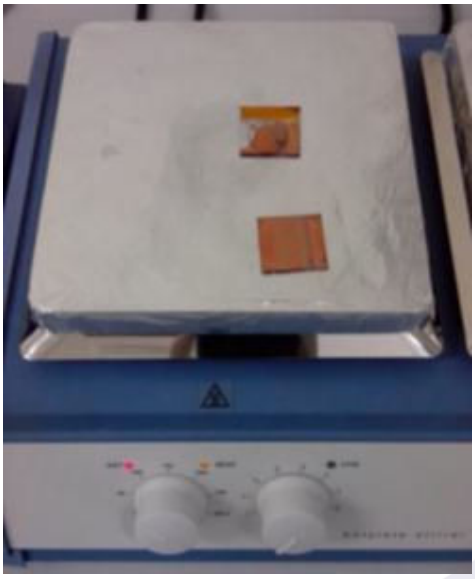

Figure 3.14: Preheating procedure

Finally, the device was completed by successive deposition of gold (Au) layer by using sputter coater with the setting of 40mA power for 200 sec, resulting 100nm thickness. The complete reference cell is shown as Figure 3.15:

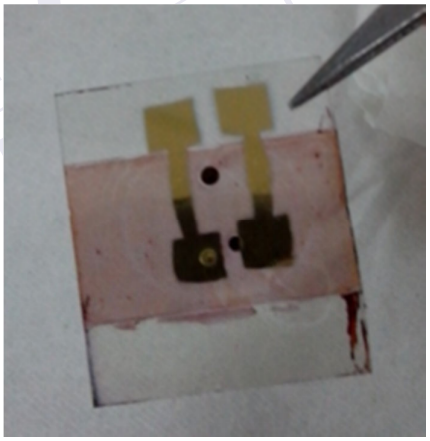

Figure 3.15: Actual device production

The process flow of the reference cell fabrication can be summarized as following graphical Figure 3.16.

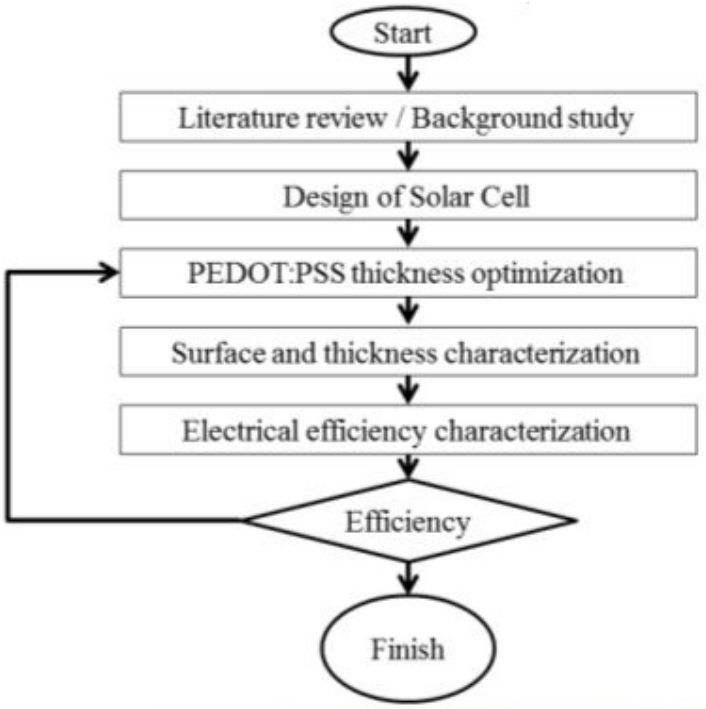

(a)

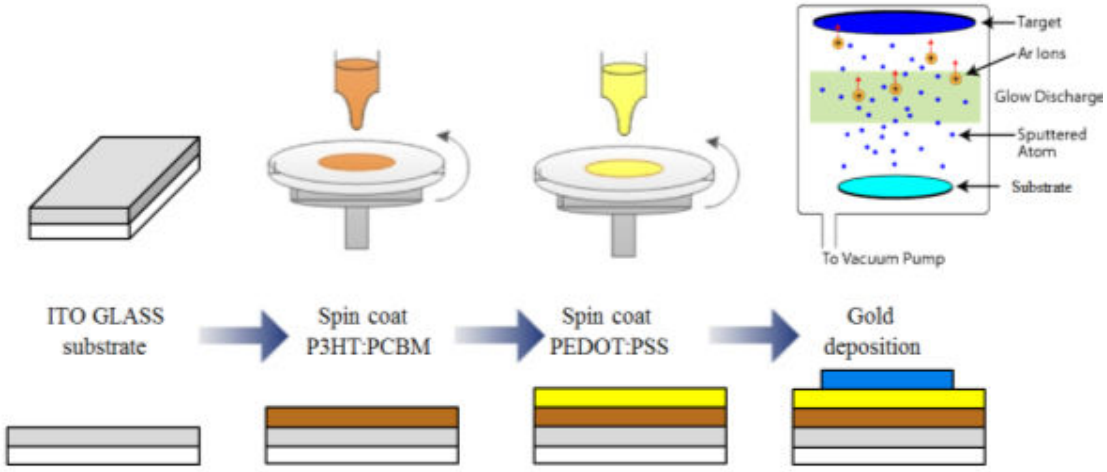

(b)

Figure 3.16: (a) Overall process flow of organic solar cells (b) Graphical images of simplified process flow

REFERENCES

[1] A.-E. Becquerel, "Mémoire sur les effets électriques produits sous l'influence des rayons solaires," *Comptes Rendus*, vol. 9, no. 567, p. 1839, 1839.

[2] W. G. Adams and R. Day, "The Action of Light on Selenium.," *Proceedings of the Royal Society of London*, vol. 25, no. 171–178, pp. 113–117, 1876.

[3] R. S. Ohl, "Light-sensitive electric device," *U.S Patent 2,402,662*, 1946.

[4] D. Chapin, C. Fuller, and G. Pearson, "A New Silicon p-n Junction Photocell for Converting Solar Radiation into Electrical Power," *Journal of Applied Physics*, vol. 25, no. 5, pp. 676–677, 1954.

[5] E. Drury et al., "Solar Energy Technologies," vol. 2, pp. 10–1 – 10–60, 2013.

[6] G. Chamberlain, "Organic solar cells: a review," *Solar Cells*, vol. 8, no. 1, pp. 47–83, 1983.

[7] C. W. Tang, "Two-layer organic photovoltaic cell," *Applied Physics Letters*, vol. 48, p. 183, 1986.

[8] N. Sariciftci, L. Smilowitz, A. Heeger, F. Wudl, and others, "Photoinduced electron transfer from a conducting polymer to buckminsterfullerene," *Science*, vol. 258, no. 5087, pp. 1474–1476, 1992.

[9] G. Yu and A. J. Heeger, "Charge separation and photovoltaic conversion in polymer composites with internal donor/acceptor heterojunctions," *Journal of Applied Physics*, vol. 78, no. 7, pp. 4510–4515, 1995.

[10] E. Perzon et al., "Design, synthesis and properties of low band gap polyfluorenes for photovoltaic devices," *Synthetic metals*, vol. 154, no. 1, pp. 53–56, 2005.

[11] M. Al-Ibrahim, O. Ambacher, S. Sensfuss, and G. Gobsch, "Effects of solvent and annealing on the improved performance of solar cells based on poly (3-hexylthiophene): Fullerene," *Applied physics letters*, vol. 86, no. 20, pp. 201120–201120, 2005.

[12] Y. Liang et al., "For the bright future—bulk heterojunction polymer solar cells with power conversion efficiency of 7.4\%," *Advanced Materials*, vol. 22, no. 20, pp. E135–E138, 2010.

[13] T. Jeranko, H. Tributsch, N. Sariciftci, and J. Hummelen, "Patterns of efficiency and degradation of composite polymer solar cells," *Solar energy materials and solar cells*, vol. 83, no. 2, pp. 247–262, 2004.

[14] Z. Hu, J. Zhang, Z. Hao, and Y. Zhao, "Influence of doped PEDOT: PSS on the performance of polymer solar cells," *Solar Energy Materials and Solar Cells*,

vol. 95, no. 10, pp. 2763–2767, 2011.

[15] G.-H. Kim, H.-K. Song, and J. Y. Kim, "The effect of introducing a buffer layer to polymer solar cells on cell efficiency," *Solar Energy Materials and Solar Cells*, vol. 95, no. 4, pp. 1119–1122, 2011.

[16] J. Kettle, H. Waters, M. Horie, and S. Chang, "Effect of hole transporting layers on the performance of PCPDTBT: PCBM organic solar cells," *Journal of Physics D: Applied Physics*, vol. 45, no. 12, p. 125102, 2012.

[17] S. Sapp, S. Luebben, Y. B. Losovyj, P. Jeppson, D. Schulz, and A. Caruso, "Work function and implications of doped poly (3, 4-ethylenedioxythiophene)-co-poly (ethylene glycol)," *Applied physics letters*, vol. 88, no. 15, pp. 152107–152107, 2006.

[18] B. C. Thompson and J. M. Fréchet, "Polymer-fullerene composite solar cells," *Angewandte Chemie International Edition*, vol. 47, no. 1, pp. 58–77, 2008.

[19] J. Birks, "Excimers," *Reports on Progress in Physics*, vol. 38, no. 8, p. 903, 1975.

[20] J.-M. Nunzi, "Organic photovoltaic materials and devices," *Comptes Rendus Physique*, vol. 3, no. 4, pp. 523–542, 2002.

[21] F. Lindholm, J. Fossum, and E. Burgess, "Application of the superposition principle to solar-cell analysis," *Electron Devices, IEEE Transactions on*, vol. 26, no. 3, pp. 165–171, 1979.

[22] C. J. Brabec et al., "Origin of the open circuit voltage of plastic solar cells," *Advanced Functional Materials*, vol. 11, no. 5, pp. 374–380, 2001.

[23] M. A. Green, "Solar cell fill factors: general graph and empirical expressions," *Solid-State Electronics*, vol. 24, no. 8, pp. 788–789, 1981.

[24] A. Luque and S. Hegedus, *Handbook of photovoltaic science and engineering*. Wiley. com, 2011.

[25] E.-K. Park, M. Choi, J.-H. Jeun, K.-T. Lim, J.-M. Kim, and Y.-S. Kim, "The effect of metal oxide nanoparticle concentrations in PEDOT: PSS layer on the performance of P3HT: PCBM organic solar cells," *Microelectronic Engineering*, 2013.

[26] H. Kim et al., "Electrical, optical, and structural properties of indium-tin-oxide thin films for organic light-emitting devices," *Journal of Applied Physics*, vol. 86, no. 11, pp. 6451–6461, 1999.

[27] Y. Wang, W. Wei, X. Liu, and Y. Gu, "Research progress on polymer heterojunction solar cells," *Solar Energy Materials and Solar Cells*, vol. 98, pp. 129–145, 2012.

[28] D. Trivedi and H. Nalwa, "Handbook of organic conductive molecules and polymers," *Handbook of Organic Conductive Molecules and Polymers*, vol. 2, 1997.

[29] B. Yin et al., "Buffer layer of PEDOT: PSS/graphene composite for polymer solar cells," *Journal of nanoscience and nanotechnology*, vol. 10, no. 3, pp. 1934–1938, 2010.

[30] "Atomic Force Microscope." [Online]. Available: http://www.nisenet.org/node/3449. [Accessed: 29–12-2013].

[31] P. Peumans, S. Uchida, and S. R. Forrest, "Efficient bulk heterojunction photovoltaic cells using small-molecular-weight organic thin films," *Nature*, vol. 425, no. 6954, pp. 158–162, 2003.